Photodegradation of Some Dyes Over Ce/FSM-16 Catalyst Under Solar Light

Ying Wu · Shiqing Liu · Yongfu Zuo · Junjie Li · Jiaqiang Wang

Abstract Ce doped FSM-16 (Ce/FSM-16) was synthesized by templating method and its photoactivity for the degradation of methyl violet, safranine T, fuchsin basic and methylthionine chloride under solar light was studied for the first time. Ce/FSM-16 had very high surface area ($863\ m^2\ g^{-1}$) and pore volume ($0.73\ cm^3\ g^{-1}$). Doping cerium ions appears important in bringing about sunlight photocatalytic activity. The photoactivity of Ce/FSM-16 is comparable with that of Degussa P25 under solar light. By contrast, undoped FSM-16 exhibited very strong adsorption capacity for these dyes, but did not exhibit significant photoactivity for them. The degradation of dyes catalyzed by Ce/FSM-16 under solar light followed a radical-type mechanism.

Keywords Photocatalyst · Ce/FSM-16 · Solar light · Degradation of dyes · Adsorption

1 Introduction

Synthetic dyes are toxic refractory chemicals, which can generate intensive color and is hazardous to the environment. Due to the large degree of organics present in these molecules and stability of modern textile dyes, conventional biological treatment methods are ineffective for their decolorization and degradation [1]. This led to the study of other effective methods. Recent studies have demonstrated that heterogeneous photocatalysis using TiO_2 as photocatalyst appears as the most emerging destructive technology [2]. But, large band gap energy (3.2 eV) for anatase TiO_2 (excitation wavelength <387.5 nm) limits its practical application under the condition of natural solar light [3]. To develop more solar light efficient catalysts, there is an urgent need to develop photocatalytic systems, which are able to operate effectively under visible light irradiation. Therefore, the possible use of visible light has recently drawn much attention. A number of systems have been reported to serve as candidates for this application recently. They include transition-metal doped TiO_2 [4], nitrogen-doped TiO_2 [5] and the photosensitization degradation of dye pollutants [6, 7]. Furthermore, chromium containing mesoporous silica molecular sieves (Cr-HMS) [8] and transition metal (Cr, V, and Fe) based titania loaded MCM-41 materials have tested positive for degradation of organics in visible light. In particular, the chromium substituted MCM-41 loaded with TiO_2 (TiO_2/Cr-Ti-MCM-41) was found to achieve the highest degradation rates of formic acid and 2,4,6-trichlorophenol [8]. Transition metal incorporated titania–silica aerogels with high surface area were also found highly active for degradation of gas phase acetaldehyde utilizing visible light [3, 9].

The vast majority of photocatalytic investigations employ TiO_2. But nowadays, there are several examples of transition metal incorporated mesoporous silicates (without TiO_2) such as chromium containing mesoporous silica molecular sieves (Cr-HMS) [10], transition metal oxide/silica aerogels (Co/SiO_2, Ni/SiO_2, Mn/SiO_2, Cu/SiO_2, V/SiO_2, Fe/SiO_2 and

Y. Wu · J. Li · J. Wang (✉)
Department of Applied Chemistry, Key Laboratory of Medicinal Chemistry for Natural Resource, Ministry of Education, Yunnan University, Kunming 650091, P.R. China
e-mail: jqwang@ynu.edu.cn

S. Liu
Provincial Key Laboratory of Rural Energy Engineering, Yunnan Normal University, Kunming 650092, P.R. China

Y. Zuo
The Environmental Monitoring Station of Dali, Dali 671000, P.R. China

Cr/SiO$_2$) [9], cobalt incorporated Al-MCM-41 (Co-Al-MCM-41) [11]. Although the value of the rate constant is certainly higher for the same reaction when performed with Degussa P25 TiO$_2$ compared with them, the catalysts have reasonable activity both in visible and in UV light are expected [11]. The highly dispersed transition metal oxides incorporated within the framework of zeolites and molecular sieves show unique reactivities not only for various catalytic reactions, but also for photocatalytic reactions under UV light irradiation, furthermore under visible-light irradiation [12]. Therefore, it is interesting to develop transition metals doped other mesoporous materials which can exhibit reasonable activity both in visible and in UV light.

Folded sheet mesoporous material (FSM-16), having one-dimensional pores with uniformly sized mesopores of cylindrical-like nature, has high porosity and large surface area ($\sim$1,000 m^2/g). FSM-16 is composed of honeycomb-like hexagonal channels and is used as highly promising model adsorbents for fundamental adsorption studies [13]. On the other hand, FSM-16 and MCM-41 have the same hexagonal arrangement of cylindrical nanopores and characteristic thin pore wall structure [14], but they were formed by different mechanisms. FSM-16 had higher thermal and hydrothermal stability than MCM-41 [14, 15] and HSM [16], leading modified FSM-16 widely used in catalysis fields. For example, cobalt-modified mesoporous FSM-16 silica (Co/FSM-16) was employed to dehydrogenate methanol to formaldehyde [17]. Besides, the titania-grafted FSM-16 sample was used as photocatalyst for photobleaching of rhodamine-6G and for oxidation of R-terpineol [18]. However, there is no report on the modified FSM-16 without loading with titania for the photodegradation of dyes under visible light irradiation so far as we know.

Recently, the incorporation of Ce into the framework of MCM-41 (Ce-MCM-41) was synthesized and found that Ce incorporated in MCM-41 can impart dual catalytic activity in heterogeneous acid as well as redox catalysis [19]. Furthermore, Ce-MCM-41 exhibited good activity and selectivity for catalytic acylation of alcohols, thiols, phenols and amines [20], as well as the catalyst exhibited high substrate (cyclohexane) conversion and good product (cyclohexanol) selectivity and it can be reused once with almost the same activity [21]. Moreover, Ce ions doped TiO$_2$ was developed to photodegrade dye molecule (X-3B) [22]. Therefore, it was suggested a good possibility to apply Ce ions to dope mesoporous FSM-16 for the first time as a photocatalyst. Herein we report that Ce ions incorporated FSM-16 (Ce/FSM-16) acts as an efficient photocatalyst for the degradation of four organic dyes: methyl violet (MV), safranine T (ST), fuchsin basic (FB), and methylthionine chloride (MC) under solar light. For comparisons, parallel experiments were also performed to monitor the photocatalytic behavior of undoped FSM-16 and TiO$_2$.

2 Experimental

2.1 Materials

Four dyes, methyl violet, safranine T, fuchsin basic, and methylthionine chloride were used without further purification and all of them were analytical grade. Their molecular formulas, λ_{max} and molecular structures were listed in Table 1.

2.2 Synthesis of Photocatalysts

FSM-16 was synthesized with a process modified from ref [23] by using hexadecyltrimethylammonium bromide [C$_{16}$H$_{33}$ (CH$_3$)$_3$N$^+$Br$^-$] as a template. A brief description of the procedure is as follows: Kanemite was synthesized by calcinations of Na$_2$SiO$_3$ · 9H$_2$O (0.13 mol) at 972 K for 6 h, followed by dispersion in 50 cm^3 water with stirring at room temperature for 3 h. The wet kanemite was filtered off, dispersed in 20 cm^3 of a 0.1 mol dm^{-3} C$_{16}$H$_{33}$ (CH$_3$)$_3$N$^+$Br$^-$ aqueous solution, and heated at 343 K for 3 h under stirring in a 50 cm^3 flask. Then the pH of the suspension was adjusted to 8$\sim$9 by adding 2 mol dm^{-3} HCl aqueous solution during the heating and the suspension was left at 343 K for a further 3 h with stirring. After cooling to room temperature, the solid products were separated from the solutions by filtration. The filtered solid products were washed thoroughly with 50 cm^3 water for five times and dried at 353 K to yield silicate/organic complexes. The calcination was carried out by slowly increasing temperature from room temperature to 823 K in air for 2 h and heating at 823 K for 6 h to remove the organic fraction. A white powder sample was obtained.
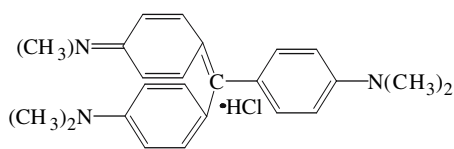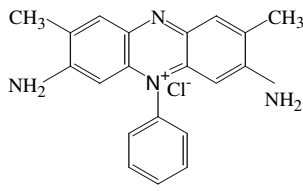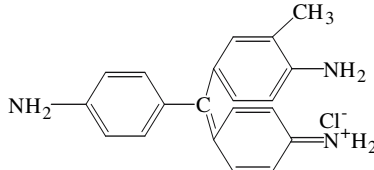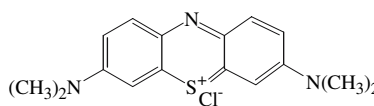
Ce/FSM-16 with 8 wt.% Ce^{3+} solid powder was synthesized by following the same procedure with preparation of FSM-16 by adding 1 mol dm^{-3} (1.6 cm^3) Ce(NO$_3$)$_3$ aqueous solution slowly after adjusting the pH of the suspension. A pale yellow powder sample was obtained.

2.3 Characterizations

Low angle X-ray powder diffraction (XRD) experiments were conducted on a D/max-3B diffractometer with Cu Kα radiation (40 kV, 30 mA). The scans were made in the 2θ range 1$\sim$10° (2θ) with a scan rate of 0.5°/min.

Pore size distributions, BET surface areas, and pore volumes were measured by nitrogen adsorption/desorption using a NOVA 2000e gas sorption analyzer (Quantachrome Corp.). Prior to the analysis, the samples were degassed at 150 °C for 1 h.

Table 1 Description of four dyes

Name of dye	Molecular formulas	λ_{max} (nm)	Molecular structures
MV[a]	$C_{24}H_{28}N_3Cl$	582.0	
ST[a]	$C_{21}H_{21}ClN_4$	513.5	
FB[a]	$C_{20}H_{20}ClN_3$	535.0	
MC[a]	$C_{16}H_{18}ClN_3S$	663.5	

[a] MV: methyl violet, ST: safranine T, FB: fuchsin basic, MC: methylthionine chloride

UV-Vis diffuse reflectance spectra were measured at room temperature in air on a Shimadzu UV-2401PC photometer over the range from 200 nm to 800 nm.

FT-IR measurements were performed on a Thermo Nicolet AVATAR FT-IR 360 instrument. Potassium bromide pellets containing 0.5% of the catalysts were used in FT-IR experiments and 32 scans were accumulated for each spectrum in transmission, at a spectral resolution of 4 cm^{-1}. The spectrum of dry KBr was taken for background subtraction.

2.4 Photocatalysis Studies

The reactions of the photocatalytic decolorization of four dyes (MV, ST, FB and MC) were carried out in a 50 cm^3 glass beaker containing 25 cm^3 of a model solution and 25 mg of photocatalyst under direct solar light between 10 a.m. and 2 p.m. where the solar intensity fluctuations were minimal. On a sunny day, the temperature of environment varied proportionally less, with the daily recordings between a high of 26 °C and a low of 20 °C. The solar radiation energy is $16.28 \sim 16.50$ MJ m^{-2} when there is relatively clearly sky in Kunming city, Yunnan Province of China [24]. All of the photocatalysis experiments were carried out on sunny days.

Dye solutions were stirred in the dark for 120 min and make sure no change in dye concentration due to adsorption before photocatalysis. The control experiments were also conducted under solar light without catalyst to measure any possible direct photolysis of these dyes. Because of the shadowing effect [4], the optional catalyst loading on the dyes of 1 g dm^{-3} was employed throughout the present study. After the systems reached the adsorption balance they were exposed for 3 h under solar light. Laboratory film was used to seal the beaker so that the volume of the solutions decreased little after the experiment. The solutions were mixed with a magnetic stirrer during the reaction process. The initial concentration of each solution was equal to 50 mg dm^{-3} with pH 6. Samples were analyzed after centrifugation (1,500 rpm for 10 min). The color removal of the dye solution was determined with the absorbance value at the maximum of the absorption spectrum for each dye by monitoring UV/Vis spectrum over $200 \sim 800$ nm. All the absorbance-concentration standard curves of four dyes aqueous solution were obtained using this apparatus.

3 Results and Discussion

3.1 Structural Analysis of the Catalysts

The low angle XRD patterns of the sample are shown in Fig 1. From the patterns, the sample exhibited several
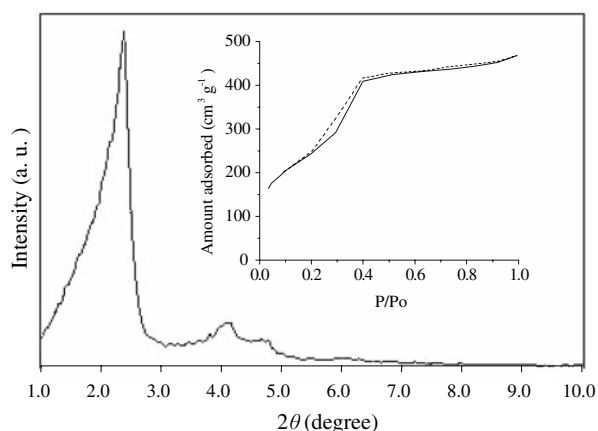
Fig. 1 XRD patterns and N$_2$ adsorption/desorption isotherms (Inset) of Ce/FSM-16

Fig. 2 UV-Vis absorption spectra of FSM-16 and Ce/FSM-16

diffraction lines in the low 2θ region, clearly indicating that the sample have a regular hexagonal structure which is in good agreement with reported literatures [14, 25].

Inset of Fig. 1 shows the nitrogen adsorption isotherms of the product. The stepwise increase in adsorption at P/P$_0$ between 0.1 and 0.4 due to filling nitrogen within the mesopores became steeper in the sample which indicated narrower pore size distribution. It was type IV isotherms of the IUPAC classification, indicating that the sample was typical mesoporous material. This is also supported by the high BET surface areas (863 m^2 g^{-1}), pore volume (0.73 cm^3 g^{-1}) and average pore diameter (32.6 Å). Both XRD and N$_2$ adsorption isotherms of the resulting sample are coincident with those found in the ref. [14, 23].

The diffuse reflectance UV-Vis spectroscopy was known to be a very sensitive probe for the identification and characterization of metal ion coordination and its existence in the framework and/or in the extra-framework position of metal containing zeolites [19]. The diffuse reflectance UV-Vis spectra of FSM-16 and Ce/FSM-16 were given in Fig. 2 and both of them show a peak with a maximum at ca. 258 nm, but different from spectra of FSM-16, the spectra of Ce/FSM-16 exhibited another absorption band around 309 nm (overlapped with the absorption band at 258 nm) which may be due to charge transfer from O^{2-} to Ce^{4+} [21]. The metal charge transfer spectra depends on the ligand field symmetry surrounding the Ce center, and the electronic transitions from oxygen to cerium require higher energy for a tetra-coordinated Ce^{4+} than for a hexa-coordinated one [20]. Therefore, it may be inferred that the presence of a strong absorption around 258–309 nm and the absence of any absorption band at 400 nm for Ce/FSM-16 sample was due to the presence of one type of well-dispersed Ce^{4+} species (presumably in a tetra-coordinate environment) [19]. Interestingly, the UV-Vis spectrum of Ce/FSM-16 is very similar to that of Ce/
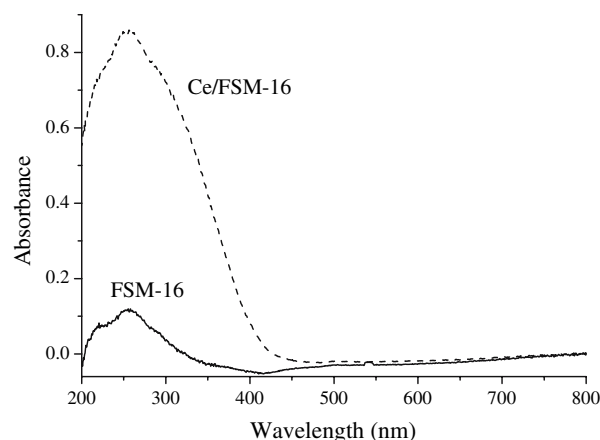
MCM-41 [21]. Clearly, the incorporation of Ce^{3+} significantly increased the absorption in UV range compared with undoped FSM-16. Moreover, the absorption edge of Ce/FSM-16 is shifted (to 420–500 nm) with decreasing band gaps, thus justifying why it can be potentially good candidate for performing photochemical reactions under solar light.

FT-IR transmittance spectra of the samples were measured to investigate structural information of nanoparticles and hydroxyl group on the particle surface and were recorded between 400 cm^{-1} and 4,000 cm^{-1} in trandmission mode using pressed KBr pellets (Fig. 3). The absorption peaks at 462, 799 and 1,083 cm^{-1} are ascribed to bond bending vibration, symmetric bond stretching vibration and asymmetric bond stretching vibration of Si–O–Si [26]. However, after the incorporation of Ce into the framewoek of FSM-16, the shifts of the bands from 1,083 cm^{-1} to 1,097 cm^{-1} and 462–469 cm^{-1} (Si–O–Ce) were observed which generally are considered an indication of the incorporation of Ce into the framework of FSM-16 [21]. In the hydroxyl region (3,000 $\sim$ 3,500 cm^{-1}), the
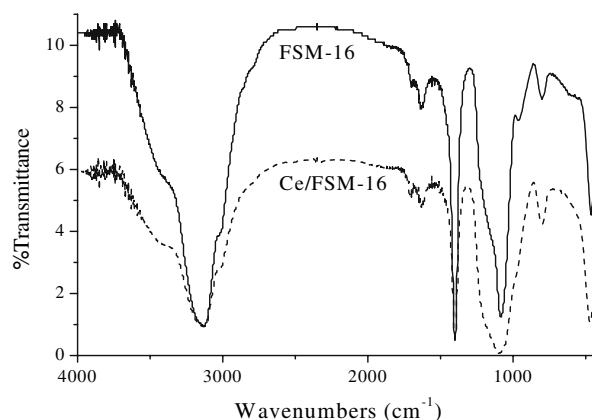
Fig. 3 FT-IR spectrum of FSM-16 and Ce/FSM-16

broad band is observed at ca. 3,131 cm^{-1} for FSM-16 and Ce/FSM-16.

3.2 The Evaluation of Photocatalytic Activity

After reaching adsorption balance (120 min in the dark), the variations for the concentrations of the studied dyes are summarized in Table 2. It is clear that both FSM-16 and Ce/FSM-16 have very strong adsorptions for four dyes. Undoped FSM-16 exhibited much higher adsorption capacity than Ce/FSM-16, but did not exhibit significant photoactivity for dyes.

Figure 4 shows the degradation UV-Vis profile of MV, ST, FB and MC. For example, the absorption bands of MV decreased rapidly and nearly vanished after 180 min under solar light but having a slight hypochromic shift, indicating the appearance of some N-de-ethylation during the photocatalytic oxidation of MV [27].

The effects of direct photolysis of four dyes without photocatalyst are also listed in Table 2. It is seen that the degradation yields of MV, FB and MC in the absence of photocatalyst are less than 4%, but the degradation yield of ST by the direct photolysis is significant with a degradation yield of 11%. Hence, in order to obtain the real photodegradation yield due to the photocatalysis in the presence of photocatalysts, the decreases of the dye concentration because of the adsorption and direct photolysis should be deducted. The decrease due to adsorption can be deducted after the adsorption equilibrium was achieved. Therefore, photodegradation yield is defined as:

$$\text{photodegradation yield} = \frac{(C_o - C_a - C_b)}{C_o} \times 100$$

C_o is the initial concentration, C_a is the concentration after photodegradation under solar light, and C_b is the decrease concentration because of the direct photolysis.

Based on the above definition, the photodegradation yields using FSM-16 and Ce/FSM-16 as photocatalysts are included in Table 2. Blank experiments indicate that the direct photolysis of MV is negligible when illuminated with solar light in the absence of catalysts. Therefore, MV was used to evaluate the photocatalytic activity of Ce/FSM-16. Figure 5 shows the photodegradation profile of MV with 50 mg dm^{-3} aqueous solution loaded 1 g dm^{-3} catalyst. The photodegradation yield of Ce/FSM-16 was compared with those of FSM-16 and Degussa P25. Within 150 min of solar light irradiation, 4, 64, and 61% of MV in an aqueous dispersion were degraded by FSM-16, Ce/FSM-16, and P25, respectively. The results demonstrate that the photocatalytic activity of Ce/FSM-16 is comparable with that of Degussa P25 under solar light and FSM-16 did not exhibit any significant activity under the same conditions. It was also observed that undoped FSM-16 did not exhibit significant activity for ST, FB, MC and MV. By contrast, Ce/FSM-16 exhibited much higher photodegradation yield than undoped FSM-16. Particularly in Fig. 6, photodegradation yields of MV and ST are over 85% (within 180 min). The order for degradation efficiency of the four dyes is: MV > ST ~ FB > MC. An initial steep increase in the photodegradation yield of the studied dyes were observed when the irradiation time was increased up to 90 min. Beyond this point, they nearly leveled off. Different from that of the other three dyes, the photodegradation yield of MV further increased after 150 min. It reveals that the chloride group cleavage depends on its position in the molecular structure. For ST, FB and MC, the chloride being bounded to the anthraquione structure as well as the nitrogen atom containing azo bond is stable in photocatalysis. In contrast, for MV, the chloride not adjacent to azo bond is more active. It still needs further identification of the other products in order to determine which one is more reactive in photocatalysis. Similar observations have been reported by Wang who found that for chloride substituted dye, the chloride in the side chain is more active with respect to cleavage than the one connected with the benzene ring [28].

3.3 Possible Photodegradation Mechanisms

The above results indicate that Ce/FSM-16 exhibited very good photoactivity under solar light, and undoped FSM-16 had no significant photoactivity but with significant adsorption capacities for these dyes. Visible light activity

Table 2 Summary of direct photolysis yield, adsorption yield, and photodegradation yield of the photocatalytic experiments (dye solutions: 25 mL, 50 mg dm^{-3}; irradiation time: 180 min)

| Name of dye	Catalysts	Direct photolysis yield (%)	Adsorption yield (%)	Photodegradation yield (%)
MV[a]	FSM-16	1	97	5
	Ce/FSM-16		84	90
ST[a]	FSM-16	11	98	Neg.[b]
	Ce/FSM-16		76	85
FB[a]	FSM-16	2	97	Neg.[b]
	Ce/FSM-16		83	83
MC[a]	FSM-16	4	95	Neg.[b]
	Ce/FSM-16		71	62

[a] MV: methyl violet, ST: safranine T, FB: fuchsin basic, MC: methylthionine chloride

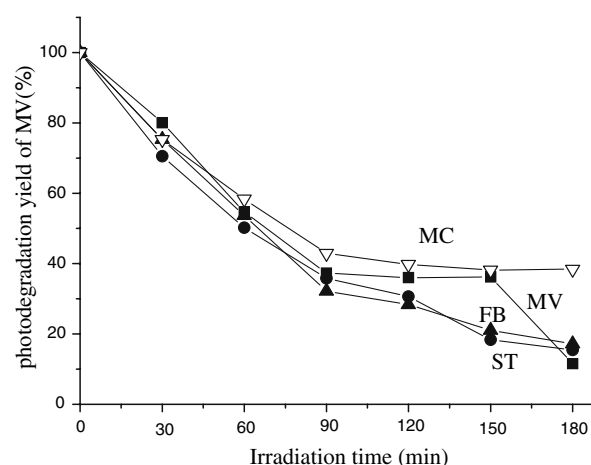[b] Neg.: negligible because of the strong adsorption and direct photolysis of dyes

Fig. 4 UV-Vis spectral changes of MV, ST, FB and MC in aqueous Ce/FSM-16 dispersions with solar light (Initial aqueous solution: 50 mg dm^{-3}, 25 cm^3; photocatalyst: 1 g dm^{-3})
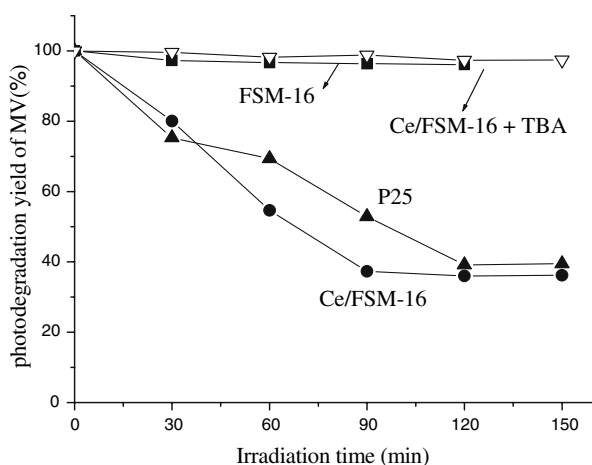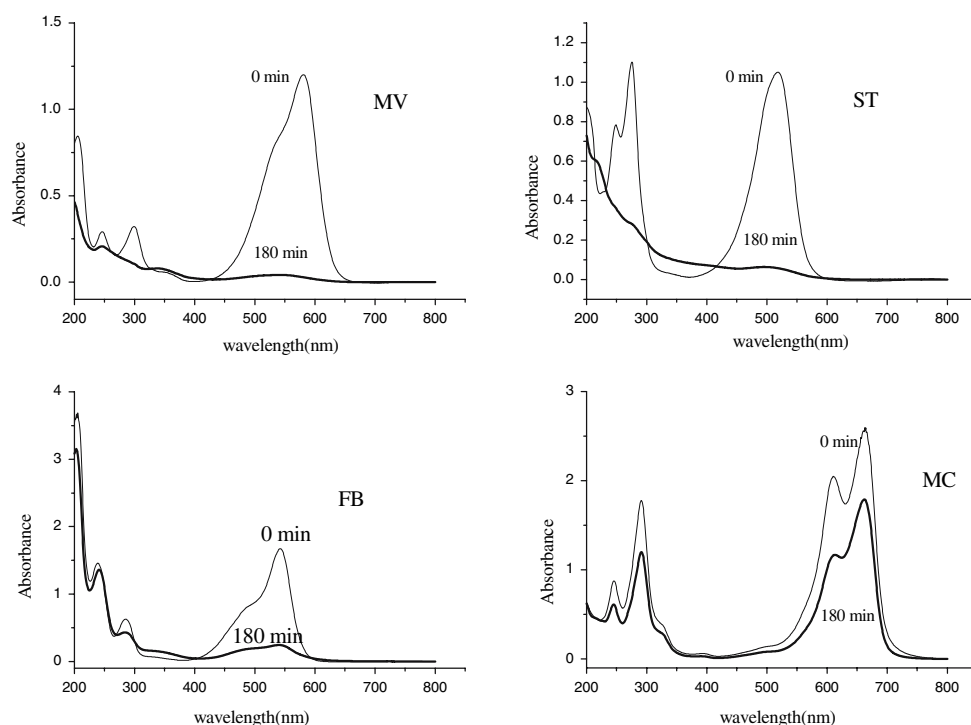

Fig. 5 Comparison of photodegradation yields of MV over Ce/FSM-16 (with and without tert-butyl alcohol), FSM-16 and Degussa P25 under solar light (Initial MV aqueous solution: 50 mg dm^{-3}; concentration of photocatalyst: 1 g dm^{-3})

Fig. 6 Comparison of photodegradation yields of MV, ST, FB and MC over Ce/FSM-16

of Ce/FSM-16 samples can be attributed to some extent to the formation of higher oxidation states of Ce upon calcination at 823 K. The pale-yellow color and UV-vis spectrum of Ce/FSM-16 inferred the formation of higher oxidation states, such as Ce^{4+} (Fig. 2). Moreover, the incorporation of Ce^{3+} significantly increased the absorption in UV range compared with undoped FSM-16 which might account for the increased efficiency of the catalyst under UV irradiation. The photoactivity probably arises due to the presence of Ce^{3+}/Ce^{4+} redox couple in the catalyst. On

the other hand, Fig. 5 clearly shows that the presence of tert-butyl alcohol (TBA), a well-known scavenger of hydroxyl radicals led to an efficient quenching of the photoactivity. This confirmed the proposition that the degradation of dyes catalyzed by Ce/FSM-16 under solar light followed a radical-type mechanism. The proposed mechanism of the charge generation happening at the heterojunction of Ce/FSM-16 could be described as follows: Ce doped mesoporous silicas are known for their tetrahedral coordination of Ce^{4+}. Such coordination allows for a special transition under solar light:

$$Ce^{4+} = O^{2-} \rightarrow Ce^{3+} = O^{-}.$$
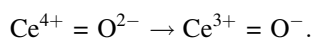
If this process happens at or near the catalyst surface, the charges can interact with the surface hydroxyl groups or adsorbed oxygen to produce hydroxyl radicals or active oxygen radicals. Thus, it has been observed that the Ce-oxide or Ce-oxide moieties in FSM-16 can exhibit efficient photocatalytic reactivity for degradation of dyes under solar light.

4 Conclusions

Ce/FSM-16 was successfully synthesized by templating method and the order for its degradation efficiency of four organic dyes (MV, ST, FB and MC) under solar light is: MV > ST $\sim$ FB > MC. By contrast, undoped FSM-16 exhibited very strong adsorption capacity for these dyes, but did not exhibit significant activity for ST, FB, MC and MV. It was also found that the photoactivity of Ce/FSM-16 is comparable with that of Degussa P25 under solar light. The degradation of dyes catalyzed by Ce/FSM-16 under solar light followed a radical-type mechanism.

References

1. Neppolian B, Choi HC, Sakthivel S, Arabindoo B, Murugesan V (2002) J Hazard Mater B 89:303
2. Konstantinou IK, Albanis TA (2004) Appl Catal B: Environ 49:1
3. Wang J, Uma S, Klabunde KJ (2004) Appl Catal B 48:151
4. Nagaveni K, Sivalingam G, Hegde MS, Madras G (2004) Appl Catal B: Environ 48:83
5. Asahi R, Morikawa T, Ohwaki T, Aoki K, Taga Y (2001) Science 293:269
6. Chen C, Li X, Ma W, Zhao J (2002) J Phys Chem B 106:318
7. Ji H, Ma W, Huang Y, Zhao J, Wang Z (2003) Chinese Sci Bull 48:2199
8. Davydov L, Reddy P, France P, Smirniortis PG (2001) J Catal 203:157
9. Wang J, Uma S, Klabunde KJ (2004) Micropor Mesopor Mat 75:143
10. Yamashita H, Katsuhiro Y, Ariyuki M, Higshimoto S, Che M, Anpo M (2001) Chem Comm 5:435
11. Rodrigues S, Uma S, Martyanov IN, Klabunde KJ (2004) J Photochem Photobiol A: Chem 165:51–58
12. Ohshiro S, Chiyoda O, Maekawa K, Masui Y, Anpo M, Yamashita H (2006) Comptes Rendus Chimie 9:846–850
13. Tozuka Y, Sasaoka S, Nagae A, Moribe K, Oguchi T, Yamamoto K (2005) J Colloid Interf Sci 291:471
14. Inaki Y, Yoshida H, Kimura K, Inagaki S, Fukushima Y, Hattori T (2000) Phys Chem Chem Phys 2:5293
15. Chen CY, Xiao SQ, Davis ME (1995) Microporous Mater 4:1
16. Elkordy A, Forbes T, Barry W (2002) Int J Pharma 247:79
17. Ghattas MS (2006) Micropor Mesopor Mat 97:107
18. Aronson BJ, Blanford CF, Stein A (1997) Chem Mat 9:2842
19. Laha SC, Mukherjee P, Sainkar SR, Kumar R (2002) J Catal 207:213
20. Kadgaonkar MD, Laha SC, Pandey RP, Kumar P, Mirajkar SP, Kumar R (2004) Catal Today 97:225
21. Yao W, Chen Y, Min L, Fang H, Yan Z, Wang H, Wang J (2005) J Mol Catal A: Chem 246:162
22. Xie Y, Yuan C (2003) Appl Catal B: Environ 46:251
23. lnagaki S, koiwai A, Suzuki N, Fukushima Y, Kuroda K (1996) Bull Chem Soc Jap 69:1449
24. Li M, Huang HB, Wang RZ, Wang LL, Yang WM, Cai WD (2005) Appl Therm Eng 25:1614
25. Katoh M, Takao H, Abe N, Tomida T (2001) J Colloid Interf Sci 242:294
26. Li W, Yao Y, Wang Z, Zhao J, Zhao M, Sun C (2001) Mater Chem Phys 70:144
27. Li J, Chen C, Zhao J, Zhu H, Orthman J (2002) Appl Catal B: Environ 37:331
28. Wang Y (2000) Wat Res 34:990